

Equilibrium, kinetic, and thermodynamic applications for methylene blue removal using *Buxus sempervirens* leaf powder as a powerful low-cost adsorbent

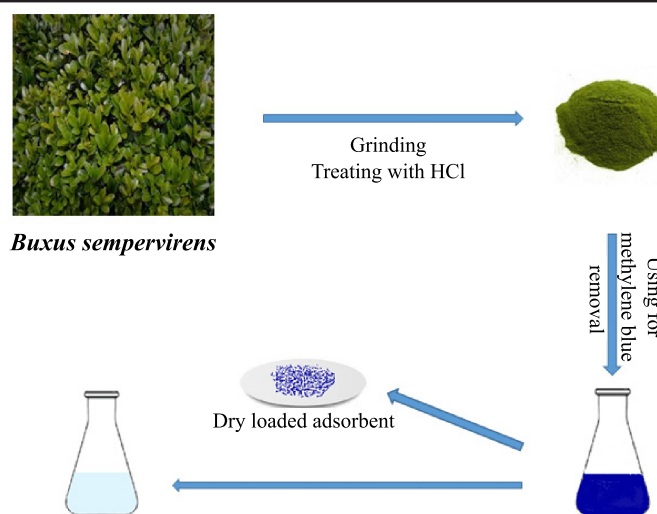
Mohammadreza Rahman-Setayesh, Ahmad Rahbar Kelishami*, Hadi Shayesteh

Research Lab for Advanced Separation Processes, Faculty of Chemical, Petroleum and Gas Engineering, Iran University of Science and Technology (IUST), Tehran, Iran

HIGHLIGHTS

- An effective adsorbent was applied for removing MB dye.
- Adsorption kinetic, isotherm, and thermodynamic were studied in detail.
- The adsorbent exhibited high adsorption capacity for the MB dye.

GRAPHICAL ABSTRACT



ARTICLE INFO

Article history:

Received 06 November 2019

Revised 12 January 2020

Accepted 15 January 2020

Keywords:

Dye

Boxwood

Biosorbent

Water treatment

ABSTRACT

In this work, methylene blue adsorption using the unconventional, natural, and low-cost adsorbent, *Buxus sempervirens* (Boxwood) leaf powder (BLP), was studied. Several experiments were conducted for the investigation of different process variables. Also different techniques such as XRF, XRD, SEM, FT-IR and N_2 adsorption-desorption analysis were applied for the characterization of BLP. Adsorption kinetic models showed that the pseudo-second-order by $R^2 = 0.999$ was well adapted. Two isotherms models, Langmuir and Freundlich, were selected to check of the amount of color removal. Methylene blue (MB) maximum adsorption capacities can attain 384.61 mg.g^{-1} from the Langmuir isotherm. The values of ΔG^0 for adsorption of MB onto BLP ranges from -19.44 to $-24.07 \text{ kJ.mol}^{-1}$, demonstrating that the adsorption process was spontaneous and irreversible. The removal of dye was considerably increased by increasing the temperature, which suggested that the adsorption process was endothermic. All results indicate that BLP can be feasibly employed for the elimination of MB from an aqueous solution.

* Corresponding author: Tel.: +9821-77451505 ; Fax: +9821-77451505 ; E-mail address: ahmadrahbar@iust.ac.ir

DOI: 10.22104/JPST.2020.3909.1160

1. Introduction

Due to their harmful effects, the discharge of wastewaters containing pollution, such as dye, heavy metal, and oil, into the environment is an important matter for many forms of life. Dyes, even at low concentrations, are a source of pollution due to the chemical oxygen demand of the effluents and increasing toxicity [1-3]. Textile, leather, paper-plastic, food, and cosmetic industries generate considerable amounts of colored wastewaters. It is reported that 0.7×10^6 tons of dyestuff are produced annually in commercially available dyes [4-6]. Methylene blue (MB) is utilized for coloring cotton, wool, silk, and paper. Profuse sweating and vomiting are among the main harmful effects of MB if ingested through the mouth. It can cause eye burns and respiratory disorders leading to a short period of labored breathing [7-9]. Because of the harmful effects on the environment and human life, the elimination of dyes from wastewaters is an essential and important task.

There are a lot of methods that have been used for the elimination of dyes such as integrated chemical-biological removal [10], membrane process [11], photocatalytic removal [12], electrochemical removal [13], as well as coagulation and flocculation processes [14-16]. Among these methods, adsorption is a useful technique because it has design cost, flexibility in the process, high efficiency, and is insensitivity to toxic solutes [17]. To reduce the cost of wastewater treatment, biosorbents, mineral, natural and waste materials have been used in many studies. These materials are abundantly available, can readily be used without any pretreatment step or activation procedure, and don't need any regeneration step, unlike expensive materials such as activated carbon.

Buxus sempervirens (Boxwood), a type of flowering plant in the genus *Buxus*, is endemic to southern Europe and southwest Asia, including Iran and northwest Africa [18,19]. Several natural adsorbents have been considered for methylene blue removal from wastewater such as *Platanus orientalis* leaf powder [4], *Salix babylonica* (Weeping willow) leaves powder [2], *Apium graveolens* [20], *Carica papaya* wood [21], Grape Peel [22], *Chlorella pyrenoidosa* and *Spirulina maxima* [23] and modified bamboo [24].

Boxwood leaves as a cheap adsorbent for the decontamination process, have not yet been reported

in the literature. Because of the abundance of alkaloids existing in their steroidal, Boxwood leaves show some interesting behavior. Different studies have been reported about the medicinal properties and chemical constituents of *Buxus sempervirens* [25-28].

The focus of this research was to study the ability of Boxwood, as a low-cost material, in the adoption of MB from a wastewater solution using parameters that affect the adsorption process (adsorbent dosage, initial MB concentration, contact time, temperature, and pH). Boxwood leaves were characterized by Fourier transform infrared spectroscopy (FT-IR), scanning electron microscope (SEM) images, and Brunauer–Emmett–Teller (BET) analysis.

2. Materials and methods

2.1. Materials

Boxwood leaves were collected from the campus of IUST University. The following steps were taken to prepare the adsorbent: first, the leaves were washed using hot deionized water (DI) and then dried in an oven for 24 h at 100 °C. Secondly, the dried leaves were then crushed and the produced Boxwood leaf powder (BLP) was sieved. A stock solution (1000 mg.L^{-1}) of methylene blue (MW 373.9 g.mol^{-1}), $\text{C}_{16}\text{H}_{18}\text{ClN}_3\text{S}$, was prepared from the Merck Company. This dye dissociates into reduced ions (CH^+) and intense molecular cation (C^+) in the aqueous solutions.

2.2. Characterization of BLP

The specific surface area and total pore volume of the BLP sample was analyzed by a BET (N_2 adsorption-desorption) analyzer (Micromeritics Instrument Corporation). A scanning electron micrograph (VEGA TESCAN) and Fourier transform infrared spectroscopy spectrophotometer in the range $500\text{-}4000 \text{ cm}^{-1}$ based on the KBr pressed disk technique (Shimadzu 8400s) were applied to portray the surface morphology and identify the chemical components of the BLP, respectively. Also, the point of zero charges, pH_{pzc} , obtained by adding 0.01 M NaCl as an electrolyte whose surface has a net charge of zero, was measured by adding 0.01 M NaCl as an electrolyte and by plotting $\text{pH}_f - \text{pH}_i$ vs. pH_i . The point at which the pH_f was equal to the pH_i was set as pH_{pzc} [29,30].

2.3. Experiments

Many batch adsorption experiments for the investigation of different process variables including the dosage of adsorbent, contact time, MB concentration, pH and temperature were performed. Initial pH adjustment included either HCl or NaOH solutions concentration. Before adding the adsorbent, every run of the experiments was tested two times and the average of the results was used in the data analysis. At constant temperature, the reaction mixture was stirred at 140 rpm on a stirrer (ROTAMIX-SHP10) for the desired time. All samples were centrifuged (EBA 20-Hettich, Germany) at 6000 rpm for 10 minutes to prevent any solid particles remaining in the liquid phase. In this work, a UV-Vis spectrophotometer (Shimadzu UV-1800, Japan, at 664 nm) was used to determine the MB concentration.

The Eqs. (1) and (2) calculated the amount of dye adsorbed (q_e , mg.g⁻¹) and removal efficiency, Re (%), on the surface of BLP:

$$q_e = (C_0 - C_t) V/S \quad (1)$$

$$Re = (C_0 - C_e)/C_0 \quad (2)$$

where C_0 and C_t are the initial and final concentrations of MB (mg.L⁻¹), respectively, V is the volume of solution (L), and S is the amount of adsorbent (g).

2.4. Experiment models

2.4.1. Kinetic models

Kinetic models can help determine whether the adsorption mechanism is chemical adsorption or polyphase catalysis. The pseudo-second-order (PSO) and intraparticle diffusion (IPD) models were analyzed to illustrate the adsorption mechanism. Two kinetic model were given as Eqs. (3) and (4) [31,32].

$$\frac{dq_t}{dt} = k(q_e - q_t)^2 \quad (3)$$

$$q_e = k_p t^{1/2} + C \quad (4)$$

in which q_e and q_t (mg.g⁻¹) are the adsorbed values at equilibrium time and at time t (min), k (g.mg⁻¹.min⁻¹) is the pseudo-second order equilibrium rate constant, k_p is the model rate constant (mg.min^{-1/2}.g), and C is the intercept determining an estimate of the boundary layer thickness.

2.4.2. Isotherm models

To describing the adsorption process at the solid-liquid interface, the adsorption isotherms were done in the initial dye concentration ranging from 10-400 mg.L⁻¹ and temperature of 25 °C. The Langmuir and Freundlich isotherms were applied to evaluate the adsorbent surface properties and adsorption behaviors. The equations of the mentioned isotherms are given by Eqs. (5) and (6) [6,33,34].

$$1/q_e = 1/(K_a q_m C_e) + 1/q_m \quad (5)$$

$$\ln q_e = \ln K_F + (1/n) \ln C_e \quad (6)$$

In the equations above, q_e (mg.g⁻¹) is the molarity value of dye adsorbed at the equilibrium which was taken at 90 min in this study, q_m (mg.g⁻¹) is the Langmuir constant demonstrating maximum adsorption monolayer capacity, and C_e (mg.L⁻¹) is the concentration of the dye solution at the equilibrium time in the solution. K_a (L. mg⁻¹) is the Langmuir constant, which is the adsorption equilibrium constant, including the affinity of binding sites. K_F ((mg.g⁻¹)/(mg.L⁻¹)^{1/n}) in Eq. (5) is the Freundlich constant, which is related to the adsorption capacity. Parameter n represents the strength of the driving force, energy, or intensity of adsorption.

2.4.3. Thermodynamic parameters

To understand that the process will occur spontaneously, entropy (ΔS^0 , J.mol⁻¹.K⁻¹), enthalpy (ΔH^0 , J.mol⁻¹) and the standard free energy (ΔG^0 , J.mol⁻¹), were used to calculate the adsorption of MB ranging from 25 to 65 °C. The relationships between ΔG^0 , ΔH^0 , and ΔS^0 were obtained using Eqs. (7) - (9) [35,36].

$$K_L = q_e/C_e \quad (7)$$

$$\Delta G^0 = RT \ln K_L \quad (8)$$

$$\ln K_L = (\Delta S^0/R) - (\Delta H^0/R)(1/T) \quad (9)$$

where T (K) and R represents the absolute temperature of the solution and the ideal gas constant (8.314 J.mol⁻¹), respectively.

3. Results and discussion

3.1. Boxwood leaf powder (BLP) characteristic

The FT-IR spectrum was used to infer the functional group of BLP, which would give insight into the organic structure. As shown in Fig. 1, the strong adsorption peak ranging from 3060 to 3700 cm^{-1} corresponds to the O–H stretching vibration of alcohols and phenols existing in cellulose, lignin and pectin structures [37]. The adsorption bands at 2920 and 1650 cm^{-1} can be interpreted as the C–H stretching vibration from CH_2 groups of cellulose and hemicelluloses and the stretching vibration of C=O groups in the BLP structure, respectively [38]. Another peak at around 1070 cm^{-1} is attributed to C–O groups in primary alcohols. Moreover, a medium band at around 1440 cm^{-1} is a result of the bending vibration of carboxylic acid groups [37].

SEM images were used to characterize the information about the surface morphology of BLP. Fig. 2 illustrates the SEM images of BLP for the time before and after the adsorption of MB. The BLP has a porous structure providing appropriate binding sites for adsorbate molecules. The porous structure of BLP was covered with MB molecules after the adsorption process. The results of potential zeta experiments indicated that the pH_{zpc} of the BLP powders was 7.7, hence at $\text{pH} > 7.7$, BLP has a negatively charged surface. The specific surface area and the total pore volume of the BLP samples were measured and evaluated by BET analysis. The corresponding results revealed that the specific surface area and total pore volume were, respectively, 11.91 $\text{m}^2\cdot\text{g}^{-1}$ and $3.3 \times 10^{-2} \text{ cm}^3\cdot\text{g}^{-1}$.

3.2. Effect of adsorbent dosage

Other researchers have shown that the amount of

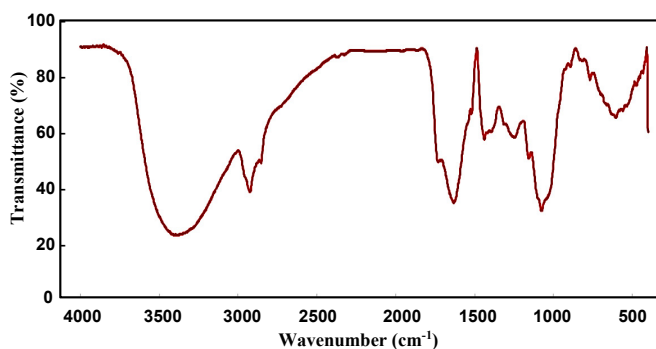


Fig. 1. FT-IR spectrum of BLP.

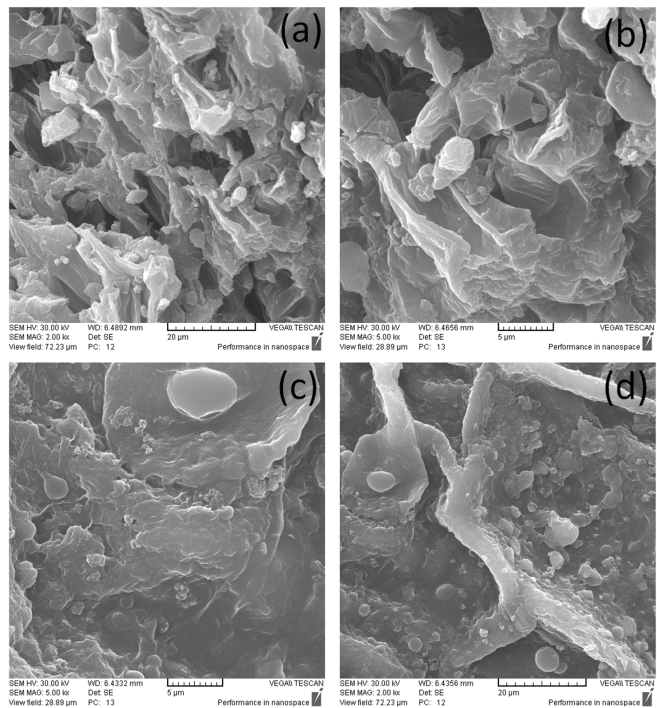


Fig. 2. SEM pictures of BLP a-b) before and c-d) after MB adsorption.

adsorbent dosage is very important in the adsorption process, and the small variation of this parameter can cause a lot of change in the amount of absorbed material. The adsorption of MB onto BLP was studied by several different amounts of adsorbent dosage (0.5–15 $\text{g}\cdot\text{L}^{-1}$) while other parameters were constant. As shown in Fig. 3, increasing the amount of adsorbent dosage from 0.5 to 1 $\text{g}\cdot\text{L}^{-1}$ decreased the amount of adsorption capacity significantly from 98 to 6 $\text{mg}\cdot\text{g}^{-1}$, but increasing from 1 to 1.5 $\text{g}\cdot\text{L}^{-1}$ produced no significant change in the amount of adsorption capacity. The maximum removal efficiency of MB on BLP was reached at an adsorbent dosage of 10–15 $\text{g}\cdot\text{L}^{-1}$. Therefore, an adsorbent dosage of 1 $\text{g}\cdot\text{L}^{-1}$ was selected as the optimum dosage for further study.

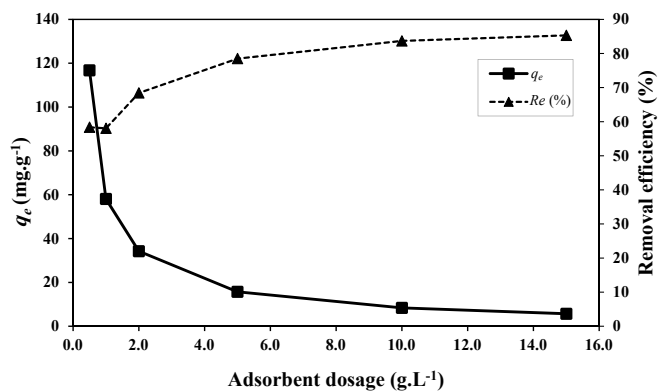


Fig. 3. Effect of adsorbent dosage on the adsorption of MB on BLP (pH: 11, temperature: 25 $^{\circ}\text{C}$, initial MB concentration: 100 $\text{mg}\cdot\text{L}^{-1}$, contact time: 24 h).

3.3. Effect of contact time

The duration of contact between adsorbent and adsorbate in the solution has been recognized as one of the most important parameters in the process. Fig. 4 shows the effect of contact time on the adsorption of MB on BLP. It seems that the adsorption process reached equilibrium after 90 min. The contact time profile of MB adsorption indicates that a smooth and continuous curve suggests the probability of a single layer of MB covering the surface of the BLP [39]. Rapid initial adsorption and slow rate adsorption indicates a two-stage kinetic behavior. Due to the vacancy of adsorbent sites of BLP and high MB concentration gradient in the solution, the adsorption rate of MB onto BLP is rapid in the first stage. The adsorption rate is sluggish in the second stage due to the coverage of adsorbent sites and low MB concentration gradient [40].

3.4. Effect of initial MB concentration on the adsorption of MB

The results obtained from the experiments showed that when initial MB concentration increased, the amount of adsorption capacity of the BLP increased (Fig. 5). There is a remarkable enhancement in MB adsorption on BLP, from 7 to 255 mg.g⁻¹, when the initial dye concentration was increased from 10 to 400 mg.L⁻¹. The initial MB concentration greatly affects the capacity of MB to adsorb onto the BLP. The driving force of concentration gradient increases at higher initial MB concentrations and therefore enhances the adsorption capacity [41].

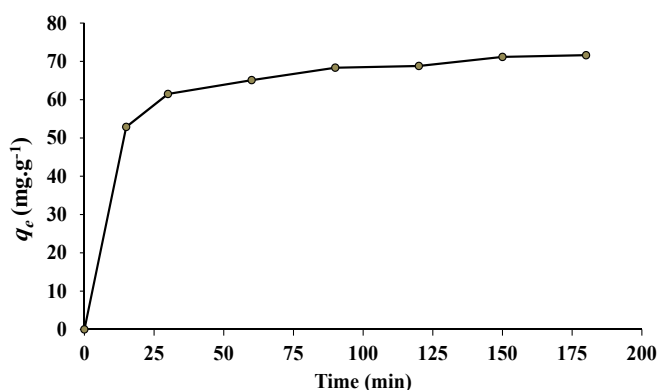


Fig. 4. Effect of contact time on the adsorption of MB on BLP, (pH:11, temperature: 25 °C, initial MB concentration:100 mg.L⁻¹, dosage: 1 g.L⁻¹).

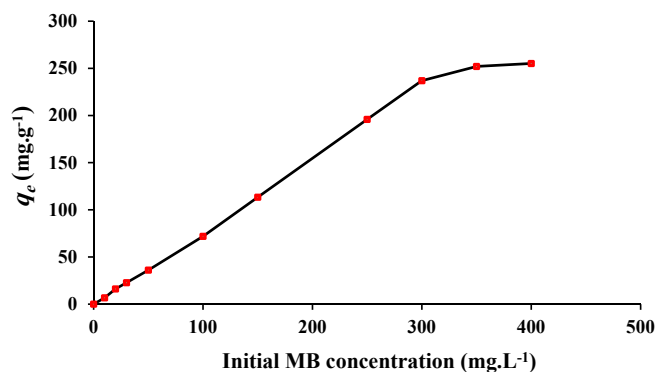


Fig. 5. Effect of initial MB concentration on the adsorption of MB on BLP, (pH:11, temperature: 25 °C, contact time: 90 min, dosage: 1 g.L⁻¹).

3.5. Effect of pH

pH plays a key role in dye adsorption, and the initial pH of the solution is an important parameter that controls the adsorption process, particularly the removal efficiency [42]. Fig. 6 shows the effect of solution pH on the adsorption of MB with BLP at 100 mg.L⁻¹ initial MB concentration with 1 g.L⁻¹ adsorbent dosage at 25 °C for 90 min. As seen in this figure, by increasing the amount of the solution pH the amount of adsorption capacity and thereby removal efficiency increase. Therefore, these changes indicate that the surface is a function of the solution pH. The FT-IR showed that BLP has of a variety of functional groups, such as hydroxyl and carboxyl, which affected by the pH. On the other hand, the pK_a of MB equals 0.04 [43]; therefore, MB-forming molecules at pK_a > 0.04 are completely ionized and it will act as a cationic species. Also, pH_{zpc} = 7.7 showed that when pH < pH_{zpc} the adsorbent surface had positive values, and repulsion between the molecules and the surface charge reduced the amount of adsorption capacity. However, when pH > pH_{zpc}, strong electrostatic attraction between the BLP surface (which the ionization of the BLP groups induces a negative charge density on) and the MB dyes (which possess positive charges) made adsorption capacity rise. Moreover, the presence of excess H⁺ ions at lower pH competing with MB cationic ions to occupy adsorption sites of BLP, can be a reason for such a smaller adsorption.

3.6. Effect of temperature

The impact of temperature changes in the range of 25 to 65 °C was investigated. Varying the temperature has

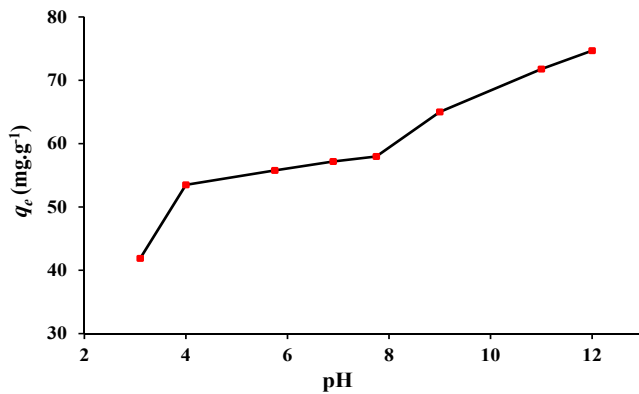


Fig. 6. Effect of pH on the adsorption of MB on BLP, (initial MB concentration: 100 mg.L⁻¹, temperature: 25 °C, contact time: 90 min, dosage: 1 g.L⁻¹).

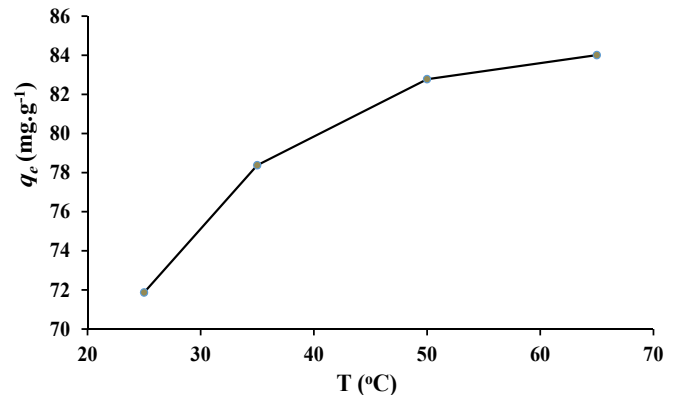


Fig.7. Effect of temperature on the adsorption of MB on BLP (pH: 11, initial MB concentration: 100 mg.L⁻¹, contact time: 90 min, dosage: 1 g.L⁻¹).

a remarkable result on the equilibrium capacity of the dye onto the adsorbent. The impact of the temperature on the MB adsorption is demonstrated in Fig. 7. It is obvious that the amount of adsorption increases with increasing temperature and reaches 84 mg.g⁻¹ when the temperature is 65 °C, suggesting that the mechanism of dye onto BLP was endothermic.

As shown in Fig. 7, increasing the amount of adsorption capacity by increasing the temperature may be either due to increasing the access to internal cavities or increasing the surface active sites on the surface of the adsorbent. Moreover, better adsorption can be related to increased locomotion of MB ions from liquid to BLP surfaces, allowing adsorption to occur more easily [44].

3.7. Adsorption kinetics

Adsorption kinetic was supported to find the influence of contact time on the adsorption process and to quantify the adsorption rate. These experiments were performed at 25 °C, and the initial MB concentration (100 mg.L⁻¹), adsorbent dosage (1 g.L⁻¹) and pH (11) were constant. Compared with the correlation coefficients (R^2) in Table 1, the R^2 of MB adsorption in the PSO model was 0.999, which was much higher than the IPD model ($R^2 = 0.894$). Therefore, the adsorption process of MB onto BLP follows the PSO kinetics with a high correlation coefficient. The values of equilibrium parameters are

reported in Table 1. Meanwhile, the $q_{e,exp}$ values of the pseudo-second-order model for MB adsorption was 73.5 mg.g⁻¹. This result is in relatively good agreement with the experiment values at 71.6 mg.g⁻¹ for the PSO model. Therefore, the adsorption of MB follows the pseudo-second-order kinetic model. This was assuming the adsorption mechanism and rate-limiting step as mainly a chemisorption process.

3.8. Adsorption equilibrium

The adsorption isotherms have a remarkable significance in the design of the adsorption process and can provide effective information such as affinity, surface properties and adsorption mechanisms. The adsorption constants and the correlation coefficients (R^2) of Langmuir and Freundlich are displayed in Table 2. In this study, the equilibrium data were simulated with Langmuir and Freundlich models. The corresponding parameters calculated from models are listed in Table 2. With the high correlation coefficient for the Langmuir model (0.9901), it can be seen that this model was the best for describing the adsorption of MB onto BLP.

The comparison between adsorption capacities of MB and different natural adsorbents is shown in Table 3. The adsorption capacity of BLP to the removal of MB (384.61 mg.g⁻¹) is higher than that for many other low-cost and natural adsorbents.

Table 1. Adsorption kinetic parameters for MB adsorption onto BLP.

Experiment	PSO kinetic			IPD kinetic		
	k (g.mg ⁻¹ .min ⁻¹)	q_e (mg.g ⁻¹)	R^2	k (mg.g ⁻¹ .min ^{-1/2})	C (mg.g ⁻¹)	R^2
$q_{e,exp}$ (mg.g ⁻¹)						
71.6	0.0022	73.5	0.999	8.45	18.76	0.894

Table 2. Adsorption isotherm parameter for MB adsorption onto BLP.

Langmuir			Freundlich		
q_m (mg.g ⁻¹)	K_a (L.mg ⁻¹)	R^2	n	K_F (mg.g ⁻¹) (L.mg ⁻¹) ^{1/n}	R^2
384.61	0.0109	0.9901	1.09	4.39	0.9794

Table 3. Comparison of the maximum adsorption of MB onto various natural and low-cost adsorbents.

Name	Value (mg.g ⁻¹)	Ref.
<i>Buxus sempervirens</i>	384.61	This study
<i>Carica papaya</i> wood	32.25	[21]
(modified celery (<i>Apium graveolens</i>	476.19	[20]
Microwave-Hydrothermal Treated Grape Peel	215.7	[22]
<i>Chlorella pyrenoidosa</i>	101.75	[23]
<i>Spirulina maxima</i>	145.34	[23]
<i>Platanus orientalis</i> leaf powder	114.94	[45]
<i>Salix babylonica</i> (Weeping willow) leaves	60.97	[2]
modified bamboo	606	[24]
Pineapple leaf powder	373.9	[37]
Broad bean peels	192.72	[46]
Jackfruit peel	285.71	[47]
Palm kernel fiber	217.95	[48]
Banana stalk waste	243.90	[49]
Coffee husks	90.1	[50]
Dehydrated peanut hull	108.6	[51]
<i>Delonix regia</i> leaf powder	186.22	[30]
Modified rice straw	208.33	[52]

3.9. Adsorption thermodynamics

The calculated thermodynamic parameters are given in Table 4. As all values of ΔG^0 are negative, it is understood that the adsorption of MB onto BLP can be a spontaneous process, confirming the affinity of MB onto BLP. Commonly, a value of $-20 < \Delta G^0$ (kJ.mol⁻¹) < 0 is described as electrostatic interaction among adsorption cavities and the adsorbate molecules. The value of ΔG^0 between -80 and 400 kJ.mol⁻¹ indicates that the adsorption process includes transferring from or charge sharing the adsorbent surface to the adsorbing molecules to make a proportionate bond (chemical adsorption) [37]. As listed in Table 4, the values of ΔG^0 for adsorption of MB onto BLP ranges from -19.44 to -24.07 kJ.mol⁻¹, demonstrating that the adsorption process was spontaneous and irreversible. The absolute

values of ΔG^0 were gradually increased with the increase of temperature, manifesting that the higher temperature strengthens the spontaneous adsorption process. The result reveals that physical adsorption is the main driving force in the first adsorption process. The positive value of ΔH^0 (14.94 kJ.mol⁻¹) confirms the endothermic of the adsorption process on MB removal onto BLP as suggested before. The positive value of ΔS^0 (116 J.mol⁻¹.K⁻¹) indicates an increase in the disorder of the MB.

Table 4. Adsorption thermodynamic parameters for MB adsorption onto BLP.

ΔG^0 (kJ.mol ⁻¹) at temperature (°C)				ΔH^0	ΔS^0
25	35	50	65	(kJ.mol ⁻¹)	(J.mol ⁻¹ .K ⁻¹)
-19.44	-20.98	-22.76	-24.07	14.94	116.06

4. Conclusion

Buxus sempervirens plant leaves (BLP) were proposed as a natural adsorbent for removal of MB from the aquatic environment. The obtained BET surface area and pore volumes were 11.91 m².g⁻¹ and 3.3×10⁻² cm³.g⁻¹, respectively. It was shown that the adsorption of MB onto BLP is favored at basic pH and higher temperatures. An increase in pH, initial MB concentration, and temperature and a decrease in adsorbent dosage led to an increase in equilibrium MB uptake. The kinetic and isotherm parameters data were fitted well by the pseudo-second-order with $R^2 = 0.999$ and Langmuir models, respectively. The findings revealed that BLP, with the maximum adsorbed amount of 384.61 mg.g⁻¹, is an excellent potential biosorbent for the removal of MB in a batch operation and it can be effectively used to treat dyeing wastewater.

References

- [1] Ö. Şahin, M. Kaya, C. Saka, Plasma-surface modification on bentonite clay to improve the performance of adsorption of methylene blue, *Appl. Clay Sci.* 116 (2015) 46-53.
- [2] A. Khodabandehloo, A. Rahbar-Kelishami, H. Shayeštah, Methylene blue removal using *Salix babylonica* (Weeping willow) leaves powder as a low-cost biosorbent in batch mode: Kinetic, equilibrium, and thermodynamic studies, *J. Mol. Liq.* 244 (2017) 540-548.

- [3] G. Çöle, M.K. Gök, G. Güçlü, Removal of basic dye from aqueous solutions using a novel nanocomposite hydrogel: N-vinyl 2-pyrrolidone/itaconic acid/organo clay, *Water Air Soil Poll.* 224 (2013) 1760.
- [4] M. Peydayesh, A. Rahbar-Kelishami, Adsorption of methylene blue onto *Platanus orientalis* leaf powder: Kinetic, equilibrium and thermodynamic studies, *J. Ind. Eng. Chem.* 21 (2015) 1014-1019.
- [5] F. Hemmati, R. Norouzbeigi, F. Sarbisheh, H. Shayesteh, Malachite green removal using modified sphagnum peat moss as a low-cost biosorbent: Kinetic, equilibrium and thermodynamic studies, *J. Taiwan Inst. Chem. E.* 58 (2016) 482-489.
- [6] H. Shayesteh, A. Rahbar-Kelishami, R. Norouzbeigi, Adsorption of malachite green and crystal violet cationic dyes from aqueous solution using pumice stone as a low-cost adsorbent: kinetic, equilibrium, and thermodynamic studies, *Desalin. Water Treat.* 57 (2016) 12822-12831.
- [7] H.R. Mahdavi, M. Arzani, M. Isanejad, T. Mohammadi, Effect of hydrophobic and hydrophilic nanoparticles loaded in D2EHPA/M2EHPA - PTFE supported liquid membrane for simultaneous cationic dyes pertraction, *J. Environ. Manage.* 213 (2018) 288-296.
- [8] T. Aysu, M.M. Küçük, Removal of crystal violet and methylene blue from aqueous solutions by activated carbon prepared from *Ferula orientalis*, *Int. J. Environ. Sci. Technol.* 12 (2015) 2273-2284.
- [9] C. Shi, F. Tao, Y. Cui, Evaluation of nitriloacetic acid modified cellulose film on adsorption of methylene blue, *Int. J. Biol. Macromol.* 114 (2018) 400-407.
- [10] M. Cheng, G. Zeng, D. Huang, C. Lai, Z. Wei, N. Li, P. Xu, C. Zhang, Y. Zhu, X. He, Combined biological removal of methylene blue from aqueous solutions using rice straw and *Phanerochaete chrysosporium*, *Appl. Microbiol. Biot.* 99 (2015) 5247-5256.
- [11] R. Zhao, Y. Li, B. Sun, S. Chao, X. Li, C. Wang, G. Zhu, Highly flexible magnesium silicate nanofibrous membranes for effective removal of methylene blue from aqueous solution, *Chem. Eng. J.* 359 (2019) 1603-1616.
- [12] N. Wang, J. Chen, J. Wang, J. Feng, W. Yan, Removal of methylene blue by Polyaniline/TiO₂ hydrate: Adsorption kinetic, isotherm and mechanism studies, *Powder Technol.* 347 (2019) 93-102.
- [13] E. Lacasa, P. Cañizares, F.C. Walsh, M.A. Rodrigo, C. Ponce-de-León, Removal of methylene blue from aqueous solutions using an Fe²⁺ catalyst and in-situ H₂O₂ generated at gas diffusion cathodes, *Electrochim. Acta.* 308 (2019) 45-53.
- [14] D. Morshedi, Z. Mohammadi, M.M. Akbar Boojari, F. Aliakbari, Using protein nanofibrils to remove azo dyes from aqueous solution by the coagulation process, *Colloid. Surface. B.* 112 (2013) 245-254.
- [15] Z. Yang, H. Yang, Z. Jiang, T. Cai, H. Li, H. Li, A. Li, R. Cheng, Flocculation of both anionic and cationic dyes in aqueous solutions by the amphoteric grafting flocculant carboxymethyl chitosan-graft-polyacrylamide, *J. Hazard. Mater.* 254-255 (2013) 36-45.
- [16] J. Xun, T. Lou, J. Xing, W. Zhang, Q. Xu, J. Peng, X. Wang, Synthesis of a starch-acrylic acid-chitosan copolymer as flocculant for dye removal, *J. Appl. Polym. Sci.* 136 (2019) 47437.
- [17] H. Cherifi, B. Fatiha, H. Salah, Kinetic studies on the adsorption of methylene blue onto vegetal fiber activated carbons, *Appl. Surf. Sci.* 282 (2013) 52-59.
- [18] K. Rushforth, *Trees of Britain and Europe*, 1st Ed., HarperCollins Pub. Ltd., 1999.
- [19] L.R. Batdorf, *Boxwood: An illustrated encyclopedia*, American Boxwood Society, 2004.
- [20] S. Mohebbali, D. Bastani, H. Shayesteh, Methylene blue removal using modified celery (*Apium graveolens*) as a low-cost biosorbent in batch mode: Kinetic, equilibrium, and thermodynamic studies, *J. Mol. Struct.* 1173 (2018) 541-551.
- [21] S. Rangabhashiyam, S. Lata, P. Balasubramanian, Biosorption characteristics of methylene blue and malachite green from simulated wastewater onto *Carica papaya* wood biosorbent, *Surface. Interfac.* 10 (2018) 197-215.
- [22] L. Ma, C. Jiang, Z. Lin, Z. Zou, Microwave-hydrothermal treated grape peel as an efficient biosorbent for methylene blue removal, *Int. J. Environ. Res. Public Health.* 15 (2018) 239.
- [23] Y.A.R. Lebron, V.R. Moreira, L.V.S. Santos, R.S. Jacob, Remediation of methylene blue from aqueous solution by *Chlorella pyrenoidosa* and *Spirulina maxima* biosorption: Equilibrium, kinetics, thermodynamics and optimization studies, *J. Environ. Chem. Eng.* 6 (2018) 6680-6690.
- [24] J.-Z. Guo, B. Li, L. Liu, K. Lv, Removal of methylene blue from aqueous solutions by chemically modified bamboo, *Chemosphere*, 111 (2014) 225-231.

- [25] J. Valnet, *Phytothérapie, traitement des maladies par les plantes*, 6^e Ed. Maloine, Paris, 1992.
- [26] F. Loru, D. Duval, A. Aumelas, F. Akeb, D. Guédon, R. Guedj, Four steroidal alkaloids from the leaves of *Buxus sempervirens*, *Phytochemistry*, 54 (2000) 951-957.
- [27] C. Fourneau, R. Hocquemiller, D. Guédon, A. Cavé, Spiroformabuxine, a novel type of *Buxus* alkaloid, *Tetrahedron Lett.* 38 (1997) 2965-2968.
- [28] X. Colom, F. Carrillo, F. Nogués, P. Garriga, Structural analysis of photodegraded wood by means of FTIR spectroscopy, *Polym. Degrad. Stab.* 80 (2003) 543-549.
- [29] M. Kosmulski, *Surface charging and points of zero charge*, CRC press, 2009.
- [30] V. Ponnusami, V. Gunasekar, S.N. Srivastava, Kinetics of methylene blue removal from aqueous solution using gulmohar (*Delonix regia*) plant leaf powder: multivariate regression analysis, *J. Hazard. Mater.* 169 (2009) 119-127.
- [31] H. Azarpira, Y. Mahdavi, D. Balarak, Removal of Cd (II) by adsorption on agricultural waste biomass, *Der Pharma Chem.* 8 (2016) 61-67.
- [32] H. Azarpira, Y. Mahdavi, O. Khaleghi, D. Balarak, Thermodynamic studies on the removal of metronidazole antibiotic by multi-walled carbon nanotubes, *Der Pharm. Lett.* 8 (2016) 107-113.
- [33] H. Shayešteh, A. Rahbar-Kelishami, R. Norouzbeigi, Evaluation of natural and cationic surfactant modified pumice for congo red removal in batch mode: Kinetic, equilibrium, and thermodynamic studies, *J. Mol. Liq.* 221 (2016) 1-11.
- [34] E. Bazrafshan, A.H. Mahvi, M. Havangi, A.H. Panahi, D. Balarak, Adsorptive removal of nitrate from aqueous environments by cupric oxide nanoparticles: kinetics, thermodynamics and isotherm studies, *Fresen. Environ. Bull.* 27 (2018) 5669-5678.
- [35] M.U. Dural, L. Cavas, S.K. Papageorgiou, F.K. Katsaros, Methylene blue adsorption on activated carbon prepared from *Posidonia oceanica* (L.) dead leaves: Kinetics and equilibrium studies, *Chem. Eng. J.* 168 (2011) 77-85.
- [36] S.K. Milonjić, A consideration of the correct calculation of thermodynamic parameters of adsorption, *J. Serb. Chem. Soc.* 72 (2007) 1363-1367.
- [37] C.-H. Weng, Y.-T. Lin, T.-W. Tzeng, Removal of methylene blue from aqueous solution by adsorption onto pineapple leaf powder, *J. Hazard. Mater.* 170 (2009) 417-424.
- [38] L.Y. Mwaikambo, M.P. Ansell, Chemical modification of hemp, sisal, jute, and kapok fibers by alkalization, *J. Appl. Polym. Sci.* 84 (2002) 2222-2234.
- [39] P.K. Malik, Use of activated carbons prepared from sawdust and rice-husk for adsorption of acid dyes: a case study of Acid Yellow 36, *Dyes Pigments*, 56 (2003) 239-249.
- [40] Y. Liu, Y. Kang, B. Mu, A. Wang, Attapulgitte/bentonite interactions for methylene blue adsorption characteristics from aqueous solution, *Chem. Eng. J.* 237 (2014) 403-410.
- [41] M. Ghaedi, M.D. Ghazanfarkhani, S. Khodadošt, N. Sohrabi, M. Oftade, Acceleration of methylene blue adsorption onto activated carbon prepared from dross licorice by ultrasonic: Equilibrium, kinetic and thermodynamic studies, *J. Ind. Eng. Chem.* 20 (2014) 2548-2560.
- [42] A. Mittal, D. Kaur, A. Malviya, J. Mittal, V.K. Gupta, Adsorption studies on the removal of coloring agent phenol red from wastewater using waste materials as adsorbents, *J. Colloid Interf. Sci.* 337 (2009) 345-354.
- [43] A. Albert, E.P. Serjeant, *Ionization constants of acids and bases: a laboratory manual*, 3rd Ed., Chapman and Hall, NY, 1984.
- [44] P. Sharma, R. Kaur, C. Baskar, W.-J. Chung, Removal of methylene blue from aqueous waste using rice husk and rice husk ash, *Desalination*, 259 (2010) 249-257.
- [45] M. Peydayesh, A. Rahbar-Kelishami, Adsorption of methylene blue onto *Platanus orientalis* leaf powder: kinetic, equilibrium and thermodynamic studies, *J. Ind. Eng. Chem.* 21 (2015) 1014-1019.
- [46] B.H. Hameed, M.I. El-Khaiary, Sorption kinetics and isotherm studies of a cationic dye using agricultural waste: broad bean peels, *J. Hazard. Mater.* 154 (2008) 639-648.
- [47] B.H. Hameed, Removal of cationic dye from aqueous solution using jackfruit peel as non-conventional low-cost adsorbent, *J. Hazard. Mater.* 162 (2009) 344-350.
- [48] A.E. Ofomaja, Sorption dynamics and isotherm studies of methylene blue uptake on to palm kernel fibre, *Chem. Eng. J.* 126 (2007) 35-43.

- [49] B.H. Hameed, D.K. Mahmoud, A.L. Ahmad, Sorption equilibrium and kinetics of basic dye from aqueous solution using banana stalk waste, *J. Hazard. Mater.* 158 (2008) 499-506.
- [50] L.S. Oliveira, A.S. Franca, T.M. Alves, S.D.F. Rocha, Evaluation of untreated coffee husks as potential biosorbents for treatment of dye contaminated waters, *J. Hazard. Mater.* 155 (2008) 507-512.
- [51] D. Özer, G. Dursun, A. Özer, Methylene blue adsorption from aqueous solution by dehydrated peanut hull, *J. Hazard. Mater.* 144 (2007) 171-179.
- [52] R. Gong, Y. Jin, J. Chen, Y. Hu, J. Sun, Removal of basic dyes from aqueous solution by sorption on phosphoric acid modified rice straw, *Dye. Pigment.* 73 (2007) 332-337.